Tunable VCSEL

Zum Seminar Optoelektronik

Autor: Connie J. Chang-Hasnain
Bereitstellung: Dipl.- Ing. Björnstjerne Zindler, M.Sc.

www.Zenithpoint.de

Erstellt: 1. Oktober 2009 – Letzte Revision: 2. Juli 2021

Inhaltsverzeichnis

Literatur

[Con] Connie J. Chang-Hasnain. Tunable VCSEL.

---

1 Originaltext

[Con]ff.

Dokument nächste Seite folgend.

Tunable VCSEL

Connie J. Chang-Hasnain, *Fellow, IEEE*

Invited Paper

***Abstract*—Vertical-cavity surface-emitting lasers (VCSELs) are now key optical sources in optical communications. Their main application is currently in local area networks using multimode optical fibers. VCSELs are also being rapidly commercialized for single-mode fiber metropolitan area and wide area network applications. The advantages of VCSEL include simpler fiber coupling, easier packaging and testing, and the ability to be fabricated in arrays. In addition, VCSELs have an inherent single-wavelength structure that is well suited for wavelength engineering. All these advantages promise to lead to cost-effective wavelength-tunable lasers, which are essential for the future intelligent, all-optical networks.**

In this paper, I will review the advances on wavelength-tunable VCSELs. I will summarize some of the early breakthroughs in wavelength engineering of VCSELs and then concentrate on the designs and properties of micromechanical tunable VCSEL.

***Index Terms*—DWDM, MAN, VCSELs, WDM.**

I. Background

I STARTED my research on vertical-cavity surface-emitting lasters (VCSELs) in 1989. One of the accepted perceptions at the time was that it was problematic to achieve the designed emission wavelength of a VCSEL; a small variation in the epitaxy could lead to a large variation in the emission wavelength. The late 1980s was also the beginning of the era of wavelength-division-multiplexed (WDM) optical fiber communications, for which wavelength precision was critical. The earlier perception of problematic wavelength control led to a common opinion that a VCSEL might not be suitable for WDM applications. Furthermore, the VCSEL emission wavelength was not at the fiber transmission window of 1.3–1.5 μm. However, I decided to focus my research on VCSELs for WDM applications, believing that wavelength control could be achieved and that what was learned about short-wavelength VCSELs would be applicable to long-wavelength VCSEL. Luckily, both have been proven correct.

In my opinion, the major advances made in the past decade toward making VCSELs for WDM applications include the demonstrations of a multiple-wavelength array, tunable VCSELs, long-wavelength VCSELs, tunable long-wavelength VCSELs, and the development of *in situ* monitoring techniques used during epitaxial growths. At the time of this writing, tremendous progress on long-wavelength VCSELs [1]–[10] and long-wavelength tunable VCSELs [11] is taking place at an extraordinarily fast pace. Many of the new developments are made by startups and the information is proprietary at present. In this paper, I will focus only on the fundamentals of tunable VCSEL.

Manuscript received October 31, 2000.

The author is with the Department of Electrical Engineering and Computer Science, University of California, Berkeley, CA 94720 USA. She is also with Bandwidth9 Inc., Fremont, CA 94538 USA (e-mail: cch@eecs.berkeley.edu).

Publisher Item Identifier S 1077-260X(00)11596-5.

II. Applications

The Internet has exploded from a scientific experiment to a daily necessity over the past ten years. The number of Internet IP addresses used, which is one measure of the size of the Internet, has been doubling every year [12]. And it took only five years for the Internet to reach 50 million users, comparing to 13 years for radio and 38 years for TV [13]. To satisfy this bandwidth explosion, new means to transmit more bandwidth were desperately sought after, particularly for wide area networks, regional and long-haul communications.

Dense wavelength division multiplexing (DWDM) [14]–[16] is the most deployed technology used to increase communication bandwidth. A DWDM system allows multiple wavelengths (each a different channel in 1530–1610-nm wavelength regime) to be transmitted in the same fiber and thus, enables service providers to gracefully upgrade their systems as demand increases. The state-of-the-art prototype system boasts a 200+ channel count and Terabits-per-second capacity over a single optical fiber. Current DWDM networks are all simple point-to-point links with various numbers of channels (typically in the tens) and the channel separation is typically 100 GHz (0.8 Å) with a trend of going to a narrower spacing of 50 and 25 GHz.

One key advantage of DWDM is the tremendous scalability of aggregate bandwidth. However, at the central offices and major hubs, the huge bandwidths transmitted through the point-to-point links must be routed efficiently to avoid severe congestion. This issue is critical as more and more broad-band links are being and will be built in the metropolitan area networks (MAN), where the demand for signal routing and switching is intense. By adding wavelength as an additional degree of freedom for routing and switching, it is possible to architect new reconfigurable all-optical switching systems with minimum congestion and high-performance cost effectiveness. This presents one exciting and new enabling application for tunable lasers.

Tunable lasers are recognized as a highly desirable component for present point-to-point DWDM systems. The immediate applications include sparing, hot backup, and fixed wavelength laser replacement, with the motivating factors being cost saving and potentially higher system reliability. Tunable lasers

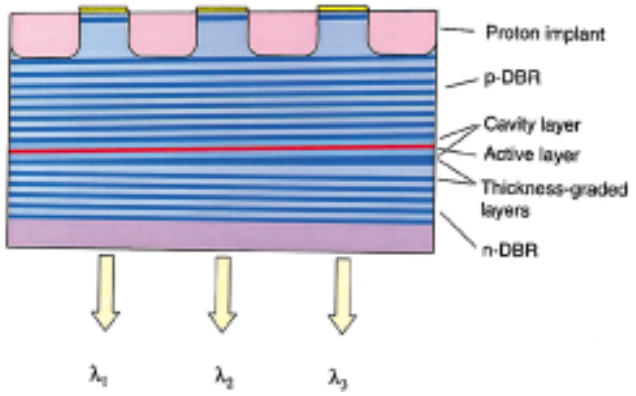

Fig. 1. Schematic of a three-wavelength VCSEL array, having a couple of layers with a graded thickness. A typical VCSEL consists of two oppositely-doped distributed Bragg reflectors (DBR) with a cavity layer in-between. In the center of the cavity layer is an active region, consisting of multiple quantum wells. Current is injected into the active region via a current guiding structure provided by a proton-implanted surrounding. The thickness gradient intentionally placed in the bottom DBRs to create a cavity thickness variation and thus led to laser wavelength variation.

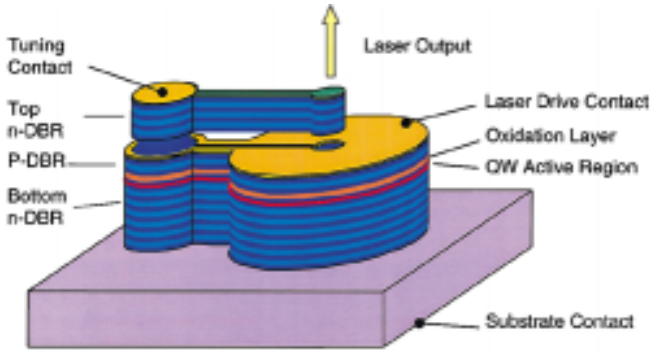

Fig. 2. Schematic of a tunable cantilever MCSEL (c-VCSEL). The device consists of a bottom n-DBR, a cavity layer with an active region, and a top mirror. The top mirror, in turn, consists of three parts (starting from the substrate side): a p-DBR, an airgap, and a top n-DBR, which is freely suspended above the laser cavity and supported via a cantilever structure. Laser drive current is injected through the middle contact via the p-DBR. An oxide aperture is formed on an AlAs layer in the p-DBR section above the cavity layer to provide efficient current guiding and optical index guiding. A top tuning contact is fabricated on the top n-DBR.

are vital, however, for enabling the future intelligent optical networks, with applications in all-optical switching and dynamically reconfigurable optical add/drop multiplexers, etc. In the following sections of this article, we hope to show that tunable VCSELs can play a pivotal role in the new intelligent optical network era with a potentially low-cost, compact and easy wavelength-locking solution.

III. Wavelength Engineering in VCSEL

The first advance made toward wavelength engineering in VCSELs, to my knowledge, was our work of multiple-wavelength VCSEL array [17], [18]. In this demonstration, my colleagues and I showed that VCSEL wavelength could be attained by design. We reported a 140-wavelength laser array by implementing a small thickness variation in four layers close to the active layer. Fig. 1 shows the concept of a three-wavelength VCSEL array, having a couple of layers with thickness gradient. The 140-wavelength array had a wavelength span of 43 nm and the laser wavelength separation was $\sim$100 GHz. This remains the largest monolithic multiple-wavelength array ever reported.

A typical VCSEL consists of two oppositely doped distributed Bragg reflectors (DBR) with a cavity layer in between. In the center of the cavity layer resides an active region, consisting of multiple quantum wells. Current is injected into the active region via a current guiding structure either provided by an oxide aperture or proton-implanted surroundings [19]–[25]. The thickness gradient intentionally placed in the bottom DBR in Fig. 1 created a cavity thickness variation and thus led to laser wavelength variation.

Our first demonstration stimulated other techniques to make monolithic multiple-wavelength VCSEL arrays. The techniques include MBE growth on a patterned substrate [26], masked MBE [27], MOCVD on a nonplanar substrate [28], selective area MOCVD growth [29], [30], and postgrowth adjustment via etching [31].

The demonstration of multiple-wavelength VCSEL array [17], [18] was the first clear illustration of the following understandings.

1) There is typically only one Fabry–Perot (FP) wavelength within the gain spectrum and hence the FP wavelength (and not the gain peak) determines the lasing wavelength.
2) Optical thickness variation of the layers in a VCSEL changes the FP wavelength and hence lasing wavelength.
3) The position of the layer(s) with thickness variation relative to the center of the cavity (i.e., the active region) is crucial for the resulting wavelength variation. For the same amount of thickness variation, the wavelength change decreases nearly exponentially as the position of the layer(s) is moved away from the cavity center.

Following the realization of the above-mentioned VCSEL properties, a series of work on tunable VCSEL were published [32]–[37]. Among them was the first three-contact device using Peltier effect to tune the VCSEL wavelength both toward shorter (blue) and longer (red) wavelengths [32] and the first external-cavity tunable VCSEL [36]. Both reported very limited wavelength shifts, 1.8 and 0.4 nm, respectively. The reasons are simple. With the three-contact device, the attainable optical thickness variation is very small, due to a limited change of refractive index with current. As for the external-cavity device, although a very large optical thickness variation is expected, the variation is placed too far away from the cavity center to result in a significant effect.

IV. Precision Epitaxy with *In Situ* Optical Monitoring

One of the most important lessons I learned from the early VCSEL experiments was the importance of being able to control and "see" what was grown during the epitaxial deposition. Since a miscalibration by as little as 1% can result in as much as 10-nm shift of the cavity resonance wavelength, precision during epitaxy is critical to obtaining wavelength-accurate VCSELs. Conventional reflection high-energy electron diffraction (RHEED) and ion-gauge beam flux measurements were not

accurate enough, typically limited to an accuracy of several percent. Various *in situ* optical techniques were developed for growth rate calibration and for real-time growth control for both molecular beam epitaxy (MBE) and metalorganic chemical vapor deposition (MOCVD) growths over the past decade [38]–[44]. Excellent results have been reported.

There are similarities and differences among the various techniques. The selection criteria for a user may include some or all of the following: accuracy, user-friendliness, variability and stability, complexity in implementation, MBE or MOCVD specifics, suitability for a wide range of materials and structures, dependence on accurate knowledge of material parameters, etc. It is beyond the scope of this paper to perform a thorough review. However, it is important to recognize the impact that *in situ* monitoring has on manufacturability and yield for VCSELs and tunable VCSELs.

A run-to-run reproducibility of $\pm 0.3\%$ was reported using an *in situ* optical calibration system for MOCVD growth [44]. Using a simple and compact laser reflectometry developed in 1995, my research group has maintained an average growth precision of 0.15% for MBE growth [43]. This is the best long-term run-to-run epitaxy precision reported to date, to the best of my knowledge. A large variety of the different structures were grown using this technique, illustrating the versatility and dependability [45].

V. Micromechanical Tunable VCSEL

I chose a radically different approach to make a widely tunable VCSEL in 1994, after realizing the constraints of the two approaches discussed in Section III. My students and I recognized that the most effective way to achieve a large amount of optical thickness variation is to mechanically vary the VCSEL cavity. The challenge was to position the movable layer close enough to the active region to achieve a large wavelength shift, while maintaining the monolithic nature of a VCSEL. This thought process led us to our first version of micromechanical VCSEL. As a learning process, my research team proceeded to demonstrate a tunable filter [46]–[48] and detector [49]–[51] first, and finally a tunable VCSEL [52]–[61].

We demonstrated the widest continuous tuning range for a monolithic electrically pumped diode laser with milliwatt-level output [57], [58]. Subsequently, other research teams published similar findings, notably Stanford University [62]–[65], Cornell University [66], Coretek Inc. [67], [68], Tokyo Institute of Technology [69], [70], the U.S. Air force Institute of Technology [71], etc..

In this section, I will first describe our MEMS-VCSEL structure, its tuning mechanism and performance. A brief comparison of process and performance of all MEMS-VCSEL designs and a performance comparison against multisection DBR laser will be presented in Section V-D.

A. c-VCSEL Structure

Fig. 2 shows a top-emitting VCSEL with an integrated cantilever microelectromechanical structure (MEMS). This VCSEL structure is herein referred to as cantilever-VCSEL (c-VCSEL). The device consists of a bottom n-DBR, a cavity layer with an active region, and a top mirror. The top mirror, in turn, consists of three parts (starting from the substrate side): a p-DBR, an airgap, and a top n-DBR, which is freely suspended above the laser cavity and supported via a cantilever structure. Laser drive current is injected through the middle contact via the p-DBR. An oxide aperture is formed on an AlAs layer in the p-DBR section above the cavity layer to provide efficient current guiding and optical index guiding. A top tuning contact is fabricated on the top n-DBR. It is particularly important to mention that this is an electrically pumped VCSEL structure, which supports high-speed direct modulation.

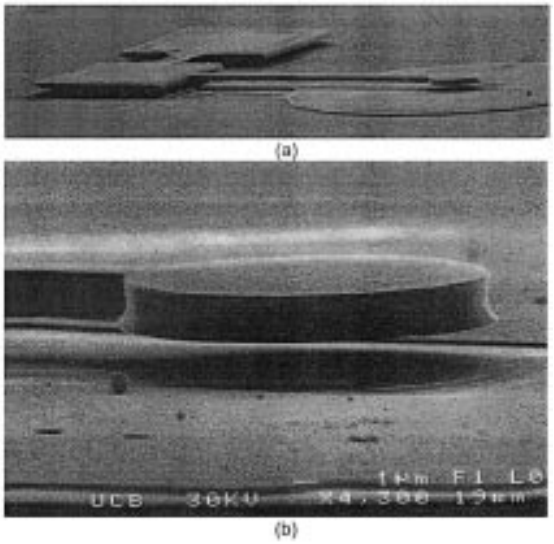

Fig. 3. SEM photos of a completed c-VCSEL. The cantilever is 3 μm wide, 100 μm long, and 3 μm thick. The head has a 10 μm diameter and the airgap is 1.4 μm thick [57].

It is worthwhile to emphasize that the entire heterostructure of the c-VCSEL was grown in one step. The heterostructure includes (starting from the substrate side) an n-GaAs–AlGaAs DBR, a cavity layer with InGaAs active region, a p-DBR (include an AlAs oxidation layer), a GaAs sacrificial layer, and a top n-DBR. Thus, a high epitaxial precision is obtained for the sacrificial layer, which translates to a highly accurate wavelength and tuning range of the c-VCSELs.

The most important processing step in fabricating a c-VCSEL is the cantilever formation and relief step, which utilizes selective etching of GaAs against AlGaAs. Fig. 3 shows the SEM photos of a completed c-VCSEL. Detailed processing steps are reported elsewhere [58]–[60]. In search of an appropriate selective etchant, we experimented with AlGaAs as sacrificial layer as well [59]. We believe it is essential to use a sacrificial layer with as low aluminum content as possible to lead to higher reliability of the mechanical structure.

B. Tuning Mechanism

Wavelength tuning is accomplished by applying a voltage between the top n-DBR and p-DBR, across the airgap. A reverse bias voltage is used to provide the electrostatic force, which attracts the cantilever downward to the substrate and shortens the airgap, thus tuning the laser wavelength toward a shorter wavelength (blue shift).

The tuning range of a MEMS-VCSEL is governed by the smallest of the following three factors: 1) the wavelength difference resulted from maximum deflection of the cantilever; 2) the minimum free spectral range (FSR), wavelength separation between two FP modes, at any tuning point; and 3) DBR or gain bandwidth. The maximum deflection is determined by the mechanical property of the cantilever as well as the capacitive nature of the attractive force. It has been derived analytically as well as simulated using complete software package [58], [60], [61]. A simple analytic approximation is given here

$$z = \frac{\pi r^2 \varepsilon}{E} \frac{2l^3}{wt^3} \frac{V^2}{(d-z)^2} \tag{1}$$

where

d	airgap size without applied voltage;
z	cantilever displacement;
V	applied voltage;
E	bulk modulus;
$r, l, w,$ and t	radius, length, width, and thickness of the cantilever, respectively.

Solving this equation, we obtain the maximum deflection, which approximates 1/3 of the airgap size (referred here as the 1/3-rule).

In fact, all MEMS using electrostatic force follow the same rule; be it a cantilever, multiple-support trampoline, or any other structures. Let us use the cantilever as an example to examine how it works. As a voltage is applied, the cantilever is attracted downwards. The displacement follows approximately V^2 dependence. As V increases further to a value corresponding to a displacement of $\sim$1/3 gap size, the attractive force cannot be balanced by the mechanical spring force, and the cantilever collapse onto the substrate. Increasing voltage further at this point results either no movement or capacitor discharge. The cantilever can be brought back to its original position when the voltage is removed if an appropriate mechanical design is used [72].

To achieve a large tuning range, given the 1/3-rule, it is natural to assume the larger the airgap the better. However, increasing the airgap leads to a longer effective cavity length, which results in a narrower FP mode separation, and thus a smaller overall tuning range. Hence, an optimum design exists.

One other consideration is the reflectivity of the p-DBR. The less the reflectivity, the larger the effect of the airgap size and hence the more tuning. However, this leads to less number of p-DBR pairs, which compromises the laser performance because of less efficient current injection and higher series resistance. We experimentally achieved a $\Delta\lambda/\lambda$ of 7% in optical filters (limited by DBR bandwidth in this case), and 3.4% for 950-nm VCSELs with very good laser performance. In principle, $>$5% $\Delta\lambda/\lambda$ can be achieved with a VCSEL, equivalent 80 nm for a 1.55-μm VCSEL.

C. Tuning Performance

The tuning spectra of a large aperture top-emitting c-VCSEL are shown in Fig. 4. A wide tuning range of 31.6 nm centered at 950 nm was achieved with the lasers under room temperature continuous-wave (CW) operation. Tuning voltage in this case

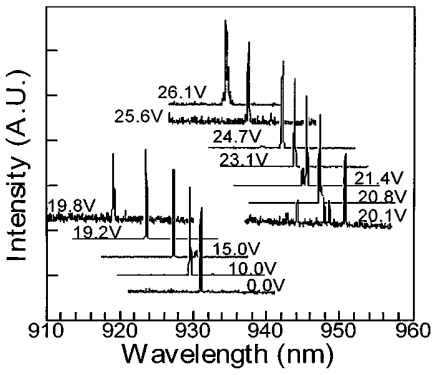

Fig. 4. The tuning spectra of a large aperture top-emitting c-VCSEL. A wide tuning range of 31.6 nm centered at 950 nm was achieved with the lasers under room temperature continuous wave (CW) operation [57].

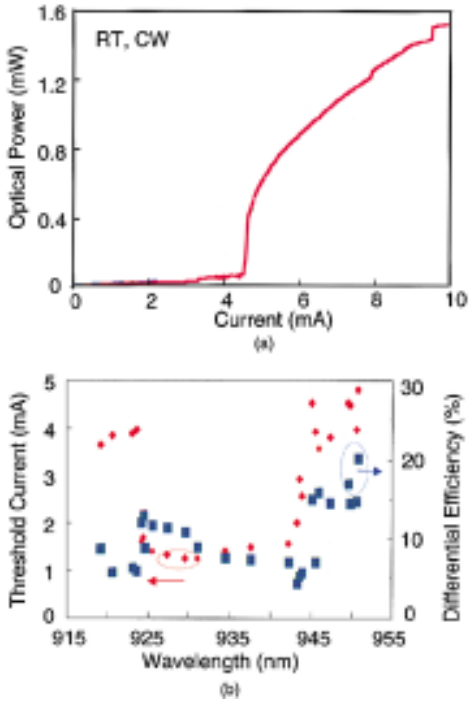

Fig. 5. (a) CW output power versus current (L–I) curve for the same device shown in Fig.4. (b) CW threshold current and differential quantum efficiency as a function of laser wavelength under room temperature CW operation.

was 26 V. As low as 5-V tuning voltage was obtained with a tunable filter and detector using a different cantilever thickness and length. Tuning power required is in 100-nW to microwatt range, as there is nearly no current flow through the tuning junction.

Fig. 5(a) shows output power versus current (L–I) curve for the same device under room temperature CW operation. Output power as high as 1.6 mW was achieved. Fig. 5(b) shows the CW threshold current and differential quantum efficiency as a function of laser wavelength. Throughout the tuning range, threshold current remained $\sim$2 mA and differential quantum efficiency was approximately 20% [58]. This represents one of the best output performance for a widely tunable diode laser.

Fig. 6 shows the measured and calculated VCSEL wavelengths as a function of the tuning voltage from a tunable VCSEL with a single transverse mode. Wavelength tuning as

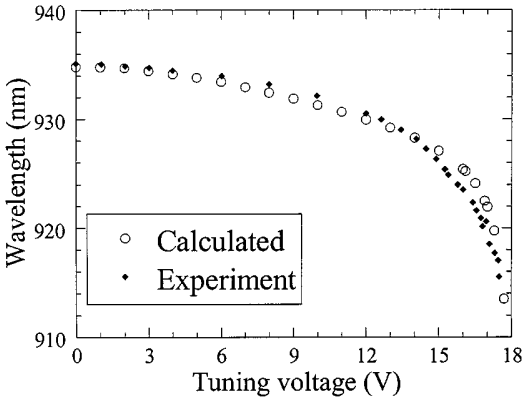

Fig. 6. Shows the measured and calculated VCSEL wavelengths as a function of tuning voltage from a tunable VCSEL with a single transverse mode. Wavelength tuning as a function of voltage was calculated using a distributed electrostatic force model to determine the airgap size, which was subsequently incorporated into a standard VCSEL optical model. Excellent agreement was achieved. No fitting parameter is used [58].

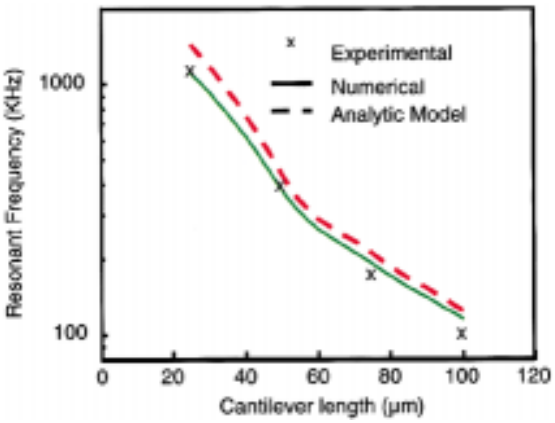

Fig. 7. The measured (x) and modeled (solid line) resonant frequencies as a function of cantilever length. Excellent agreement is obtained for between experiment and simulation. A simplified analytic solution (2) assuming concentrated force at the head is shown (dash line) for comparison [60].

a function of the voltage was calculated using a distributed electrostatic force model to determine the airgap size, which was subsequently incorporated into a standard VCSEL optical model. Excellent agreement was achieved without any fitting parameter being used. The monotonic and well-behaved tuning curve attests that a very simple wavelength locking mechanism can be sufficient to insure wavelength accuracy during tuning. This is a distinct advantage of a tunable c-VCSEL.

The transverse mode structure of a tunable VCSEL is well behaved and the same as that of a regular VCSEL [55]. The amount of index guiding and the oxide aperture size determines the number of excited transverse modes. Single-mode operation is achieved with $>$20-dB side mode suppression ratio throughout tuning range for a relatively small aperture laser [58], [60]. Single and fixed polarization was maintained throughout as well [58].

The tuning speed, like tuning voltage, is also determined by the cantilever dimensions. Tuning speed is measured to be 1–10 ms, which is fast compared to other MEMS devices because of the lightweight of the cantilever structure [60]. Fig. 7 shows the measured and modeled resonant frequencies as a function of cantilever length. Excellent agreement is obtained for between experiment and simulation. A simplified analytic solution [see (2)] assuming concentrated force at the head is shown (dash line) for comparison. Though not completely accurate, it serves as an excellent intuitive guide

$$\omega = \sqrt{\frac{k}{m}} = \sqrt{\frac{Ewt^3}{2l^3 m}}. \tag{2}$$

D. Other Tunable Diode Lasers

As mentioned earlier, there are several teams reported MEMS VCSELs or similar optical MEMS structures. The mechanical and optical designs can be grouped into three major categories: cantilever VCSEL [46]–[61], [69]–[71], membrane VCSEL [62]–[66], and a half-symmetric cavity VCSEL [67], [68]. Here, I will briefly review the membrane-VCSEL and half-symmetric VCSEL, and will discuss the similarities and differences of all three VCSELs. There is one other tunable VCSEL configuration, which utilized an optical fiber as part of the external cavity of a VCSEL [73]. Due to the fact that this approach is nonmonolithic, I shall not include in the comparisons. Finally, I will briefly compare the tunable VCSELs with multisection DBR edge-emitting lasers.

Fig. 8(a) shows the schematic of a VCSEL with a membrane-type MEMS design (referred as membrane-VCSEL). The heterostructure, starting from the substrate side, includes an n-DBR, a cavity layer with active region in the middle, a p-DBR section, an $Al_{0.85}Ga_{0.15}As$ sacrificial layer, and a top quarter-wave GaAs layer. After the epitaxy, a dielectric DBR and layer of gold are deposited on top of the wafer, which together with the top quarter-wave GaAs layer forms the top mirror. The processing steps are described elsewhere [62]–[65]. Laser emission is collected from the bottom of the substrate via the transparent GaAs substrate (referred as bottom-emitting VCSEL).

The output power and differential efficiency of the membrane-VCSELs are low (0.12 VAR $\sim$0.3 mW and 0.088 W/A), perhaps due the complicated processing, the choices of the sacrificial layer and the selective etchant. The membrane-VCSEL has a tuning range of 30 nm with the center wavelength at 965 nm, comparable to the c-VCSEL. The lasers are electrically pumped. The high Al content in the sacrificial layer may be problematic for long-term device reliability and stability.

The MEMS-VCSEL using a half-symmetric trampoline MEMS structure is shown in Fig. 8(b) (referred as HS-VCSEL). This VCSEL is an optically pumped tunable VCSEL emitting in the 1.55-μm wavelength regime. The epitaxy structure was not disclosed in the publications [67], [68]. Both top and bottom DBRs are dielectric mirrors and the substrate is etched with a via-hole to accommodate the deposition of the bottom DBR. The mechanical support structure is made of polyimide. A wide tuning range of 43 nm centered at 1550 nm was achieved with a pumping threshold of 9 mW and an efficiency of 0.1 mW/mW. Since the pumping source is another laser external to tunable VCSEL, this approach is not strictly speaking monolithic. The major advantage of optical pumping is a higher output power,

as less heat is generated at the active region. However, it is a general perception that the external optical pumping requires a highly precise optical alignment, which may be problematic for manufacturing.

The main similarity between the three MEMS-VCSEL schemes is that they tune the same way: as the tuning voltage is increased, the electrostatic force attracts the top DBR toward the substrate and the laser wavelength blue shifts. Also, the tuning range is limited by the same 1/3 rule and FP-mode competition.

The major differences include the pumping scheme, modulation scheme, chip size, and mechanical support material. The first three factors impact system designs and applications, cost, yield, and manufacturability, whereas the mechanical support material directly affect the device reliability. The fact that polyimide typically continues to outgas after curing and $Al_{0.85}Ga_{0.15}As$ is easily oxidized at room temperature raises concerns about long-term reliability.

The c-VCSEL structure was entirely epitaxially grown. Thus, the gap and the VCSEL as a whole are very precisely fabricated, which ensures wavelength and tuning range accuracy. The mechanical support is GaAs, which does not oxidize easily and leads to a higher mechanical reliability. The cantilever structure is very forgiving toward processing variations and facilitates manufacturability. The device footprint is smaller resulting a higher device yield. Due to the small structure, the tuning voltage is low and the tuning speed is fast.

It has been argued that a cantilever tuning structure could incur more excess tilt loss during tuning. Recently, we showed both experimentally and theoretically that the tilt loss in a c-VCSEL is negligible compared with the total optical loss (sum of mirror, internal, and diffraction losses) [58], [74].

There are many rapid developments in the area of widely tuned multisection DBR lasers [75]–[78]. It is beyond the scope of this paper to review and compare them in details. However, we will discuss some key features. A multisection DBR laser typically requires four or more electrodes to achieve a wide tuning range and a full coverage of wavelengths in the range. A very wide tuning range of 60–80 nm with full coverage can be achieved. The tuning characteristics is discontinuous and typically contains many steps. Knowledge of the wavelengths at which the discrete steps occur is critical for precise wavelength control (even with a wavelength locker as part of a feedback loop). As the laser drive current and heat sink temperature are varied, the step wavelengths change. As the device ages, the step wavelengths vary as well. Furthermore, as the fabrication process includes several steps of epitaxial growth, there are significant device-to-device and batch-to-batch variations. These factors make laser testing and qualification processes complicated and time consuming. Furthermore, wavelength control and locking are more complicated and may require fine adjustments for each device. The impact of these issues is volume manufacturability and cost.

One advantage of a multisection DBR laser structure is that it allows for integration of other devices such as a modulator, amplifier, and coupler. The impact of such integration on performance (such as chirp, optical feedback, and noise) and device yield is not fully explored at present. Without an integrated

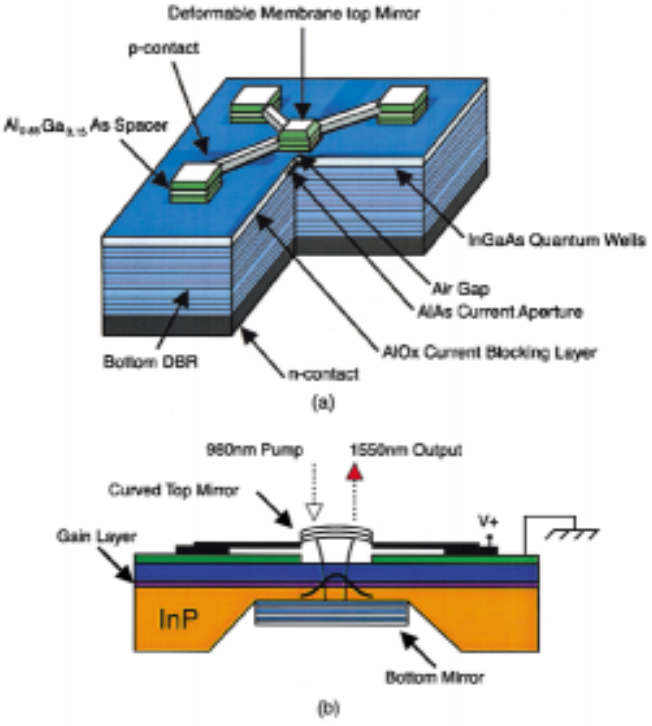

Fig. 8. (a) Schematic of a VCSEL with a membrane-type MEMS design (referred as membrane-VCSEL) [65]. (b) Schematic of a half-symmetric cavity MEMS-VCSEL by [68].

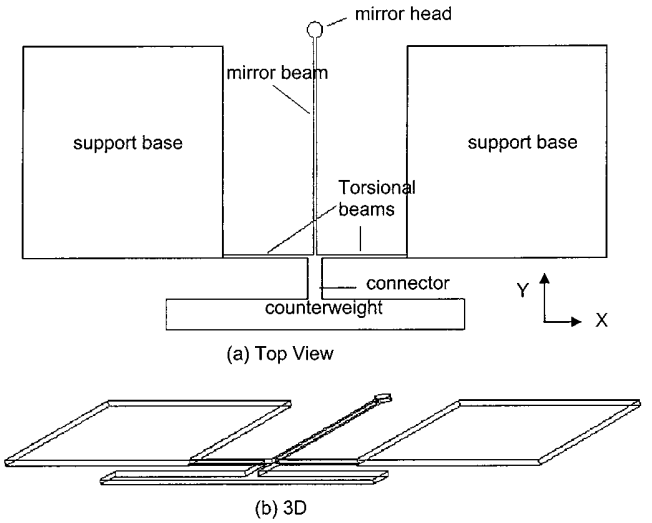

Fig. 9. Novel torsional MEMS filter. When a voltage is applied between the top and bottom DBRs, the entire structure experiences an electrostatic force pulling it towards the substrate. However, by design, the position of the center of mass lies in the counterweight; the filter head thus moves upwards whereas the counterweight moves downwards [81].

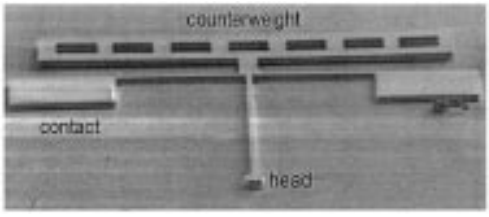

Fig. 10. SEM picture of a torsional MEMS filter [79].

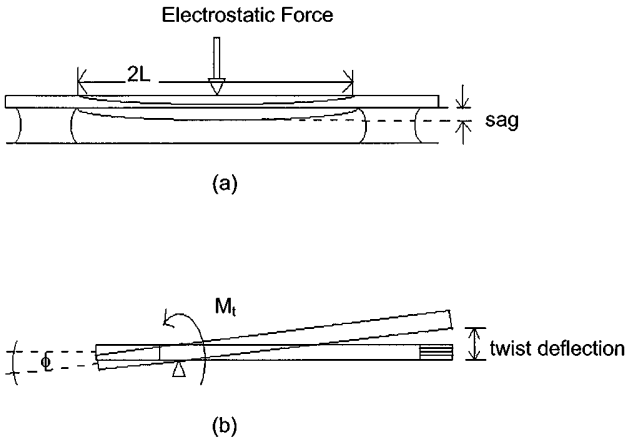

Fig. 11. Illustration of two side-views of the device (a) along x direction and (b) along y direction in Fig. 9. With the filter locating at the head, the filter wavelength increases with voltage (red-shift) [81].

modulator, the device typically cannot be directly modulated. The output power of a multisection DBR laser without an integrated semiconductor optical amplifier is typically low, in the submilliwatt level.

VI. Torsional-MEMS Filter

The 1/3 rule poses a limitation on all three MEMS-VCSEL designs mentioned above. Furthermore, the consequence of accidentally applying a voltage to tune beyond the 1/3 gap can be problematic—device damages may occur as the capacitor discharges. To solve this problem, we started looking for a method to circumvent the limitation. Recently, we started to explore a novel design using a MEM structure with a torsional arm. This design can simultaneously lead to an increase of tuning range and the elimination of the catastrophic damage when bias voltage exceeds the limit corresponding to the 1/3 gap.

The novel structure can be viewed in Fig. 9. As in the past, we first demonstrated the concept using a simple Fabry–Perot filter [79]–[81]. The epitaxial structure consists of two opposite-doped DBRs and a GaAs sacrificial layer in-between. Using similar processing steps (as for c-VCSEL), we fabricated the torsional micromechanical tunable filter. Fig. 10 shows the SEM picture of such a filter.

The optical filter functions as follows. When a voltage is applied between the top and bottom DBRs, the entire structure experiences an electrostatic force pulling it toward the substrate. However, by design, the position of the center of mass lies in the counterweight; the filter head thus moves upwards whereas the counterweight moves downwards. Fig. 11 illustrates two side views of the device. With the filter locating at the head, the filter wavelength increases with voltage (red shift). A detailed analysis and simulation can be found elsewhere [80], [81].

With increasing voltage, the filter head continues to move upward until either of the following occurs, depending upon the design. The counterweight may reach the 1/3 gap and collapse onto the substrate. Alternatively, the attraction force on the filter head becomes strong enough and causes the cantilever to bend, resulting in quadratic tuning characteristics. Either case can be designed and managed such that the catastrophic discharge does not take place at the filter head. And in principle, the discharge can be avoided by making the region underneath the edge of the counterweight electrically insulated.

TABLE I
Twist Ratios for a Number of Dvice Dimensions Calculated Using Pro/MECHANICATM [81]

Various dimensions [μms]					
cantilever width	3	3	3	5	5
mirror beam width	3	3	3	5	5
cantilever length	70	70	90	80	80
mirror beam length	190	190	210	170	170
counterweight width	25	25	30	30	30
counterweight length	300	300	300	300	300
connector width	25	15	15	25	25
connector length	25	35	30	30	40
R_T	2.08	2.18	2.35	1.32	1.41

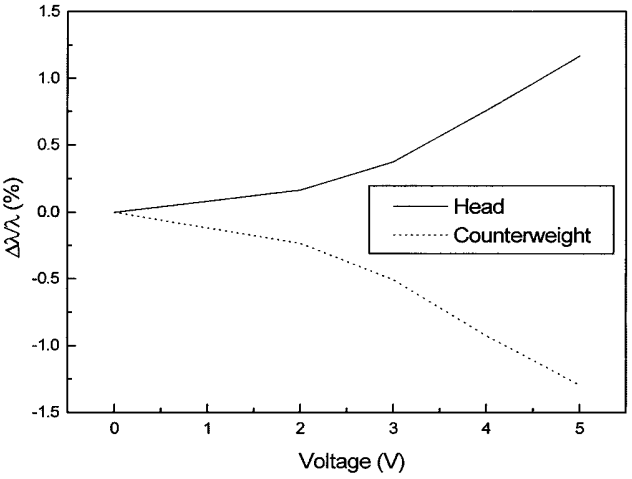

Fig. 12. The experimental performance of the torsional MEMS (T-MEMS) filter. The transmission wavelengths through the filter head and the counterweight were measured as a function of applied voltage. The transmission wavelength of the filter increases with voltage, whereas that of the counterweight decreases [79].

A major advantage of this design is an increased tuning range. By appropriately choosing the length ratio of the cantilever arm and the counterweight, a leveraging effect can be achieved, as illustrated by Fig. 11(b). We define the twist ratio R_T as

$$R_T = \frac{|\text{MaxHeadDeflection}|}{\text{MaxCounterweightDeflection}}. \tag{3}$$

Table I shows the twist ratios for a number of device dimensions calculated using Pro/MECHANICA.

The experimental performance of the torsional MEMS (T-MEMS) filter is shown on Fig. 12. The transmission wavelengths through the filter head and the counterweight were measured as a function of applied voltage. The transmission wavelength of the filter increases with voltage, whereas that of the counterweight decreases, as expected. This early result shows a continuous tuning of the transmitted light across 15 nm for 15 V of tuning voltage. At bias above 15 V, the cantilever arm begins to bend causing the filter wavelength to turn back toward the blue side. No catastrophic damage was observed. Although the design is expected to lead to a twist ratio of greater

than 1.5, we obtained a ratio of $\sim$1 only experimentally. We attribute this to processing related issues that can be overcome in the future.

The torsional MEMS design can be readily transferred to a VCSEL design leading to a wider tuning range and avoiding reliability issues caused by capacitor discharge.

VII. Conclusion

Widely tunable lasers are expected to play an important role in enabling a wide range of exciting new applications. For example, metro WDM systems based on widely tunable laser sources will be capable of providing wavelength-on-demand services because these systems will be able to set up and tear down protocol-transparent wavelength services as required, particularly by the bursty nature of data traffic. In addition, optical cross connects (OXCs), either with electrical or all-optical switch fabrics, are emerging to handle high-density optical terminations typically found at the interconnection points between long-haul and metro WDM systems. OXCs are used to groom and re-route traffic across optical tributaries. They also provide protection and restoration of the signal. Wavelength tuning capabilities will dramatically increase the degree of connectivity and number of logical connections, and will support a variety of protection and restoration methods on physical ring deployments.

The monolithic integration of MEMS and VCSEL has successfully combined the best of both devices and led to an unprecedented performance in wavelength tunable lasers. The tunable cantilever VCSELs are widely tunable, can be directly modulated at high data rates, have a simple monotonic tuning curve for easy wavelength-locking, tune at reasonably fast speed, and emit a reasonable amount of power. The most important property is that they can be batch processed and tested, essential characteristics of volume manufacturability.

Acknowledgment

This paper summarizes work contributed by many collaborators, former and present students, whose names appear in the references. The author appreciates their contributions in making the story told here an extremely exciting one. Thanks are due to future collaborators and students, who are destined to lead us to an even more fascinating place. The author wishes to acknowledge the support of NSF, DARPA, ONR, and Packard Foundation over the many years of the program, and in particular, the program managers for believing in the seemingly unlikely.

References

[1] W. Yuen, G. S. Li, R. F. Nabiev, J. Boucart, P. Kner, R. J. Stone, D. Zhang, M. Beaudoin, T. Zheng, C. He, M. Jensen, D. P. Worland, and C. J. Chang-Hasnain, "High-performance 1.6 μm single-epitaxy top-emitting VCSEL," *Electron. Lett.*, vol. 36, no. 13, pp. 1121–1123, 2000.

[2] J. Boucart, C. Stark, F. Gaborit, A. Plais, N. Bouche, E. Derouin, L. Goldstein, C. Fortin, D. Carpentier, P. Salte, F. Brillouet, and J. Jacquet, *IEEE Photon. Technol. Lett.*, vol. 11, p. 629, 1999.

[3] M. Ortsiefer, R. Shau, G. Bohm, F. Kohler, and M.-C. Amann, *Electron. Lett.*, vol. 36, pp. 437–, 2000.

[4] N. Nishiyama, S. Sato, T. Miyamoto, T. Takahashi, N. Jikutani, M. Arai, A. Matsutani, F. Koyama, and K. Iga, "First CW operation of 1.26 μm electrically pumped MOCVD grown GaInNAs/GaAs VCSEL," in *Conf. Dig. Int. Semiconductor Laser Conf.*, Monterey, CA, Sept. 2000.

[5] S. Nakagawa, E. M. Hall, G. Almuneau, J. K. Kim, H. Kroemer, and L. A. Coldren, "1.55 μm InP-lattice-matched VCSELs operating at RT under CW," in *Conf. Dig. Int. Semiconductor Laser Conf.*, Monterey, CA, Sept. 2000, pp. 151–152.

[6] S. Nakagawa, E. M. Hall, G. Almuneau, J. K. Kim, and L. A. Coldren , "Room-temperature CW operation of lattice-matched long-wavelength VCSELs," *Electron. Lett.*, vol. 36, pp. ????–????, June 2000.

[7] A. J. Fischer, J. F. Klem, K. D. Choquette, O. Blum, A. A. Allerman, I. J. Fritz, S. R. Kurtz, W. G. Breiland, R. Sieg, and K. M. Geib, "Continuous wave operation of 1.3μm vertical cavity InGaAsN quantum well lasers," in *Conf. Dig. Int. Semiconductor Laser Conf.*, Monterey, CA, Sept. 2000, pp. 7–8.

[8] M. C. Larson, C. W. Coldren, S. G. Spruytte, H. E. Petersen, and J. S. Harris, "Low threshold current continuous-wave GaInNAs/GaAs VCSELs," in *Conf. Dig. Int. Semiconductor Laser Conf.*, Monterey, CA, Sept. 2000, pp. 9–10.

[9] A. Karim, K. A. Black, P. Abraham, D. Lofgreen, Y. J. Chiu, J. Piprek, and J. E. Bowers, "Superlattice barrier 1528nm vertical cavity laser with 85°C continuous wave operation," in *Conf. Dig. Int. Semiconductor Laser Conf.*, Monterey, CA, Sept. 2000, pp. 157–158.

[10] J. A. Lott, N. N. Ledentsov, V. M. Ustinov, N. A. Maleev, A. E. Zhukov, M. V. Maximov, B. V. Volovik, and D. Bimberg, "Vertical cavity surface emitting lasers with InAs–InGaAs quantum dot active regions on GaAs substrates emitting at 1.3 μm," in *Conf. Dig. Int. Semiconductor Laser Conf.*, Monterey, CA, Sept. 2000, pp. 13–14.

[11] Bandwidth9 claims laser breakthrough. [Online]. Available: http: www.lightreading.com

[12] NetWizards.. [Online]. Available: http://www.nw.com/

[13] V. Khosla, "New ecomony tsunami, plenary talk," in *Conf. Optical Fiber Communications*, Baltimore, MD, Mar. 2000.

[14] C. A. Brackett, "Dense wavelength division multiplexing networks: Principles and applications," *IEEE J. Select. Areas Commun.*, vol. 8, no. 6, pp. 948–964, 1990.

[15] B. Mukherjee, *Optical Communication Networks*. San Francisco, CA: McGraw-Hill, 1997.

[16] G. P. Agrawal, *Fiber-Optic Communication Systems*, 2nd ed. New York: Wiley, 1997.

[17] C. J. Chang-Hasnain, M. W. Maeda, N. G. Stoffel, J. P. Harbison, L. T. Florez, and J. Jewell, "Surface emitting laser arrays with uniformly separated wavelengths," in *Conf. Dig. Int. Semiconductor Laser Conf.*, Davos, Switzerland, Sept. 1990, pp. 18–19.

[18] C. J. Chang-Hasnain, J. P. Harbison, C. E. Zah, M. W. Maeda, L. T. Florez, N. G. Stoffel, and T. P. Lee, "Multiple wavelength tunable surface emitting laser arrays," *IEEE J. Quantum Electron.*, vol. 27, no. 6, pp. 1368–1376, 1991.

[19] M. Orenstein, A. Von Lehmen, C. J. Chang-Hasnain, N. G. Stoffel, L. T. Florez, J. P. Harbison, J. Wullert, and A. Scherer, "Matrix addressable vertical cavity surface emitting laser array," *Electron. Lett.*, vol. 27, no. 5, pp. 437–438, 1991.

[20] G. Hasnain, K. Tai, L. Yang, Y. H. Wang, R. J. Fischer, J. D. Wynn, B. Weir, N. K. Dutta, and A. Y. Cho, "Performance of gain-guided surface emitting lasers with semiconductor distributed Bragg reflectors," *IEEE J. Quantum Electron.*, vol. 27, pp. 1377–1385, June 1991.

[21] K. D. Choquette, K. M. Geib, C. I. H. Ashby, R. D. Twesten, O. Blum, H. Q. Hou, D. M. Follstaedt, B. E. Hammons, D. Mathes, and R. Hull, "Advances in selective wet oxidation of AlGaAs alloys," *IEEE J. Select. Topics Quantum Electron.*, vol. 3, pp. 916–926, 1997.

[22] D. L. Huffaker, L. A. Graham, H. Deng, and D. G. Deppe, "Sub-40 mu A continuous-wave lasing in an oxidized vertical-cavity surface-emitting laser with dielectric mirrors," *IEEE Photon. Technol. Lett.*, vol. 8, pp. 974–976, 1996.

[23] A. E. Bond, P. D. Dapkus, and J. D. O'Brien, "Aperture dependent loss analysis in vertical-cavity surface-emitting lasers," *IEEE Photon. Technol. Lett.*, vol. 11, pp. 397–399, Apr. 1999.

[24] C. Lei, H. Deng, J. J. Dudley, S. F. Lim, B. Liang, M. Tashima, and R. W. Herrick, "Manufacturing of oxide VCSEL at Hewlett Packard," in *1999 Dig. LEOS Summer Topical Meetings: Nanostructures and Quantum Dots/WDM Components/VCSEL's and Microcavaties/RF Photonics for CATV and HFC Systems*, San Diego, CA, July 1999.

[25] C. J. Chang-Hasnain, *Advances of VCSELs*: Optical Soc. America, 1997.

[26] W. Yuen, G. S. Li, and C. J. Chang-Hasnain, "Multiple-wavelength vertical-cavity surface-emitting laser arrays," *IEEE J. Select. Topics Quantum Electron.*, vol. 3, pp. 422–428, 1997.

[27] H. Saito, I. Ogura, and Y. Sugimoto, "Uniform CW operation of multiple-wavelength vertical-cavity surface-emitting lasers fabricated by mask molecular beam epitaxy," *IEEE Photon. Technol. Lett.*, vol. 8, no. 9, pp. 1118–1120, 1996.

[28] F. Koyama, T. Mukaihara, Y. Hayashi, N. Ohnoki, N. Hatori, and K. Iga, "Two-dimensional multiwavelength surface emitting laser arrays fabricated by nonplanar MOCVD," *Electron. Lett.*, vol. 30, pp. 1947–1948, 1994.

[29] G. G. Ortiz, S. Q. Luong, S. Z. Sun, J. Cheng, H. Q. Hou, G. A. Vawter, and B. E. Hammons, "Monolithic, multiple-wavelength vertical-cavity surface-emitting laser arrays by surface-controlled MOCVD growth rate enhancement and reduction," *IEEE Photon. Technol. Lett.*, vol. 9, pp. 1069–1071, 1997.

[30] Y. Zhou, S. Luong, C. P. Hains, and J. Cheng, "Oxide-confined monolithic, multiple-wavelength vertical-cavity surface-emitting laser arrays with a 40-nm wavelength span," *IEEE Photon. Technol. Lett.*, vol. 10, pp. 1527–1529, 1998.

[31] T. Wipiejewski, M. G. Peters, and L. A. Coldren, "Vertical cavity surface emitting laser diodes with post-growth wavelength adjustment," *IEEE Photon. Technol. Lett.*, vol. 7, pp. 727–729, 1995.

[32] C. J. Chang-Hasnain, C. E. Zah, G. Hasnain, J. P. Harbison, L. T. Florez, and N. G. Stoffel, "Tunable wavelength emission of a 3-mirror vertical cavity surface emitting laser," in *Conf. Dig. Int. Semiconductor Laser Conf.*, Davos, Switzerland, Sept. 1990, pp. 24–25.

[33] C. J. Chang-Hasnain, J. P. Harbison, C. E. Zah, L. T. Florez, and N. C. Andreadakis, "Continuous wavelength tuning of two-electrode vertical cavity surface emitting lasers," *Electron. Lett.*, vol. 27, no. 11, pp. 1002–1003, 1991.

[34] P. R. Berger, N. K. Dutta, K. D. Choquette, G. Hasnain, and N. Chand, "Monolithic Peltier-cooled vertical-cvity surface-emitting lasers," *Appl. Phys. Lett.*, vol. 59, no. 1, pp. 117–119, 1991.

[35] L. Fan, M. C. Wu, H. C. Lee, and P. Grodzinski, "10.1 nm range continuous wavelength-tunable vertical-cavity surface-emitting lasers," *Electron. Lett.*, vol. 30, no. 17, pp. 1409–1410, 1994.

[36] N. Yokouchi, T. Miyamoto, T. Uchida, Y. Inaba, F. Koyama, and K. Iga, "4 angstrom continuous tuning of GaInAsP/InP vertical-cavity surface-emitting laser using an external cavity mirror," *IEEE Photonics Technol. Lett.*, vol. 4, no. 7, pp. 701–703, 1992.

[37] C. Gmachi, A. Kock, M. Rosenberger, E. Gormick, M. Micovic, and J. F. Walker, "Frequency tuning of a double-heterojunction AlGaAs/GaAs vertical-cavity surface-emitting laser by a serial integrated in-cavity modulator diode," *Appl. Phys. Lett.*, vol. 62, pp. 219–221, 1993.

[38] N. C. Frateschi, S. G. Hummel, and P. D. Dapkus, "*In situ* laser reflectometry applied to the growth of AlxGa1–xAs Bragg reflectors by metalorganic chemical vapor deposition," *Electron. Lett.*, vol. 27, pp. 155–157, 1991.

[39] K. Bacher, B. Pezeshki, S. M. Lord, and J. S. Harris Jr., "Molecular beam epitaxy growth of vertical cavity optical devices with *in situ* corrections," *Appl. Phys. Lett.*, vol. 61, pp. 1387–1389, 1992.

[40] Y. Raffle, R. Kuszelewicz, R. Azoulay, G. Le Roux, J. C. Michel, L. Dugrand, and E. Toussaere, "*In situ* metalorganic vapor phase epitaxy control of GaAs/AlAs Bragg reflectors by laser reflectometry at 514 nm," *Appl. Phys. Lett.*, vol. 63, pp. 3479–3481, 1993.

[41] S. A. Chalmers and K. P. Kileen, "Real-time control of molecular beam epitaxy by optical-based flux monitoring," *Appl. Phys. Lett.*, vol. 63, pp. 3131–3133, 1993.

[42] Y. M. Houng, M. R. T. Tan, B. W. Liang, S. Y. Wang, and D. E. Mars, "*In situ* thickness monitoring and control for highly reproducible growth of distributed Bragg reflectors," *J. Vac. Sci. Technol. B*, vol. 12, pp. 1221–1224, 1994.

[43] G. S. Li, W. Yuen, K. Toh, L. E. Eng, S. F. Lim, and C. J. Chang-Hasnain, "Accurate molecular beam epitaxial growth of vertical-cavity surface-emitting laser using diode laser reflectivity," *IEEE Photon. Technol. Lett.*, vol. 7, no. 9, pp. 971–973, 1995.

[44] H. Q. Hou, H. C. Chui, K. D. Choquette, B. E. Hammons, W. G. Breiland, and K. M. Geib, "Highly uniform and reproducible vertical-cavity surface-emitting lasers grown by metalorganic vapor phase epitaxy with *in situ* reflectometry," *IEEE Photon. Technol. Lett.*, vol. 8, pp. 1285–1287, Oct. 1996.

[45] G. S. Li, "Wavelength selective detectors for fiber optic communications," in *Applied Physics*. Stanford, CA: Stanford Univ., 1998.

[46] E. C. Vail, M. S. Wu, G. S. Li, L. E. Eng, and C. J. Chang-Hasnain, "Highly tunable (70 nm) optical filter using GaAs DBR movable cantilevers," in *IEEE/LEOS Annu. Meeting*, Boston, MA, Nov. 1994.

[47] ——, "GaAs micromachined widely tunable Fabry–Perot filters," *Electron. Lett.*, vol. 31, pp. 228–229, Feb. 2, 1995.

[48] M. S. Wu, G. S. Li, W. Yuen, and C. J. Chang-Hasnain, "Widely tunable 1.5μm micromechanical optical filter using AlOx/AlGaAs DBR," *Electron. Lett.*, vol. 33, no. 20, pp. 1702–1703, Sept. 1997.

[49] E. C. Vail, M. S. Wu, G. S. Li, W. Yuen, and C. J. Chang-Hasnain, "A novel widely tunable detector with wavelength tracking," in *Optical Fiber Communications Conf. (OFC)*, San Diego, CA, Feb. 1995.

[50] M. S. Wu, E. C. Vail, G. S. Li, W. Yuen, and C. J. Chang-Hasnain, "Widely and continuously tunable micromachined resonant cavity detector with wavelength tracking," *IEEE Photon. Technol. Lett.*, vol. 8, no. 1, pp. 98–100, 1996.

[51] G. S. Li, W. Yuen, and C. J. Chang-Hasnain, "A wide and continuously tunable detector with uniform characteristics over tuning range," *Electron. Lett.*, vol. 33, no. 13, pp. 1122–1124, 1997.

[52] E. C. Vail, M. S. Wu, G. S. Li, W. Yuen, and C. J. Chang-Hasnain, "Tunable micromachined vertical cavity surface emitting lasers," in *Quantum Electronics Laser Science Conf.*, Baltimore, MD, May 1995.

[53] M. S. Wu, E. C. Vail, G. S. Li, W. Yuen, and C. J. Chang-Hasnain, "Tunable micromachined vertical cavity surface emitting laser," *Electron. Lett.*, vol. 31, pp. 1671–1672, Sept. 1995.

[54] E. C. Vail, G. S. Li, W. Yuen, and C. J. Chang-Hasnain, "High performance micromechanical tunable vertical cavity surface emitting lasers," *Electron. Lett.*, vol. 32, pp. 1888–1889, Sept. 1996.

[55] ——, "High performance and novel effects of micromechanical tunable vertical cavity lasers," *IEEE J. Select. Topics Quantum Electron. Semiconduct. Lasers*, vol. 3, pp. 691–697, Apr. 1997.

[56] M. Y. Li, W. Yuen, G. S. Li, and C. J. Chang-Hasnain, "High performance continuously tunable top-emitting vertical cavity laser with 20.0nm wavelength range," *Electron. Lett.*, vol. 33, no. 12, pp. 1051–1052, 1997.

[57] ——, "Top-emitting micromechanical VCSEL with a 31.6 nm tuning range," *IEEE Photon. Technol. Lett.*, vol. 10, no. 1, pp. 18–20, 1998.

[58] M. Y. Li, "Wavelength tunable micromechanical vertical cavity surface emitting lasers," in *Electrical Engineering*. Stanford, CA: Stanford Univ., 1999.

[59] M. S. Wu, "Micromachined wavelength tunable optoelectronic devices and applications in all-optical networks," in *Electrical Engineering*. Stanford, CA: Stanford Univ., 1997.

[60] E. C. Vail, "Micromechanical tunable vertical cavity surface emitting lasers," in *Electrical Engineering*. Stanford, CA: Stanford Univ., 1997.

[61] C. J. Chang-Hasnain, "Micromechanical tunable vertical cavity lasers," in *Vertical-Cavity Surface-Emitting Lasers: Technology and Applications*, J. Cheng and N. Dutta, Eds: Gordon Breach Science, 2000, pp. 279–316.

[62] M. C. Larson, B. Pezeshki, and J. S. Harris, "Vertical coupled-cavity microinterferometer on GaAs with deformable-membrane top mirror," *IEEE Photon. Technol. Lett.*, vol. 7, pp. 382–384, Apr. 1995.

[63] M. C. Larson, A. R. Massengale, and J. S. Harris, "Continuously tunable micromachined vertical cavity surface emitting laser with 18 nm wavelength range," *Electron. Lett.*, vol. 32, pp. 330–332, Feb. 15, 1996.

[64] F. Sugihwo, M. C. Larson, and J. S. Harris Jr., "Micromachined widely tunable vertical cavity laser diodes," *IEEE J. Microelectromech. Syst.*, vol. 7, no. 1, 1998.

[65] F. Sugihwo, M. C. Larson, and J. S. Harris, jr, "Simultaneous optimization of membrane reflectance and tuning voltage for tunable vertical cavity lasers," *Appl. Phys. Lett.*, vol. 72, pp. 10–12, 1998.

[66] G. L. Christenson, A. T. T. D. Tran, Z. H. Zhu, Y. H. Lo, M. Hong, J. P. Manneaerts, and R. Bhat, "Long-wavelength resonant vertical-cavity LED/photodetector witha 75–nm tuning range," *IEEE Photon. Technol. Lett.*, vol. 9, pp. 725–727, June 1997.

[67] D. Vakhshoori, P. Tayebati, C.-C. Lu, M. Azimi, P. Wang, J.-H. Zhou, and E. Canoglu, "2mW CW singlemode operation of a tunable 1550 nm vertical cavity surface emitting laser with 50 nm tuning range," *Electron. Lett.*, vol. 35, pp. 900–901, 1999.

[68] D. Vakhshoori, J.-H. Zhou, M. Jiang, M. Azimi, K. McCallion, C. C. Liu, K. J. Knopp, J. Cai, P. D. Wang, P. Tayebati, H. Zhu, and P. Chen, "C-band tunable 6mW vertical cavity surface emitting lasere," in *Proc. Conf. Optical Fiber Commun.*, Baltimore, MD, Mar. 2000.

[69] T. Amano, F. Koyama, N. Nishiyama, and K. Iga, "2×2 multiwavelength micromachined AlGaAs/GaAs vertical cavity filter array with wavelength control layer," *Jpn. J. Appl. Phys.*, vol. 39, pp. L673–L674, July 2000.

[70] T. Amano, F. Koyama, N. Furukawa, N. Nishiyama, A. Matsutani, and K. Iga, *Electron. Lett*, vol. 36, p. 74, 2000.
[71] J. A. Lott, M. J. Noble, E. M. Ochoa, L. A. Starman, and W. D. Cowan, "tunable red vertical cavity surface emitting lasers using flexible miro-electro-mechanical top mirrors," in *IEEE Int. Conf. Optical MEMS*, Kauai, HI, Aug. 2000.
[72] D. M. Bloom, "The grating light valve: Revolutionizing display technology," in *Proc. SPIE*, vol. 3013, 1997, pp. 165–171.
[73] K. Hsu, C. M. Miller, D. Babic, D. Houng, and A. Taylor, "Continuously tunable photopumped 1.3-μm fiber Fabry–Perot surface-emitting lasers," *IEEE Photon. Technol. Lett.*, vol. 10, pp. 1199–1201, 1998.
[74] M. Li and C. J. Chang-Hasnain, "Tilt loss in wavelength-tunable micromechanical vertical cavity lasers," in *Conf. Lasers Electro-Optics*, Baltimore, MD, May 1999.
[75] B. Mason, G. A. Fish, V. Kaman, J. Barton, L. A. Coldren, S. P. DenBaars, and J. E. Bowers, "Characteristics of sampled grating DBR lasers with integrated semiconductor optical amplifiers and electroabsorption modulators," in *Proc. Conf. Optical Fiber Commun.*, Baltimore, MD, 2000.
[76] H. Ishii, T. Tanobe, F. Kano, Y. Tohmori, Y. Kondo, and Y. Yoshikuni, "Broad range wavelength coverage (62.4nm) with superstructure grating DBR laser," *Electron. Lett.*, vol. 32, pp. 454–455, 1996.
[77] M. Oberg, S. Nilsson, K. Streubel, J. Wallin, L. Backborn, and T. Klinga, "74 nm wavelength tuning range of an InGaAsP/InP vertical grating assisted codirectional coupler laser with rear sampled grating reflector," *IEEE Photon. Technol. Lett.*, vol. 5, pp. 735–738, 1993.
[78] R. C. Alferness, U. Koren, L. L. Buhl, B. I. Miller, M. G. Young, T. L. Koch, G. Raybon, and C. A. Burrus, "Broadly tunable InGaAsP/InP laser based on a vertical coupler filter with 57–nm tuning range," *Appl. Phys. Lett.*, vol. 60, pp. 3209–3211, 1992.
[79] J. M. Waite, C. F. R. Mateus, S. Chase, and C. J. Chang-Hasnain, "Torsional micromechanical tunable optical filter," in *OSA Annu. Meeting*, Providence, RI, Oct. 2000.
[80] J. M. Waite, "A micromechanical red-shifting tunable vertical cavity filter," M.S. thesis, 2000.
[81] S. Chase, "A torsional micromechanical tunable vertical cavity filter," M.S. thesis, 1999.

Connie J. Chang-Hasnain (M'88–SM'92–F'98) was born in Taipei, Taiwan, R.O.C., on October 1, 1960. She received the B.S. degree in electrical engineering and computer sciences from the University of California, Davis, in 1982, and the M.S. and Ph.D. degrees in electrical engineering and computer sciences from the University of California, Berkeley, in 1984 and 1987, respectively.

She is a Professor of electrical engineering and computer sciences at the University of California, Berkeley. In November 1997, she founded Bandwidth9 Inc. to vitalize her research on tunable VCSELs into practical leading-edge products that enable ultra-high capacity and flexibility in metro-area optical networks. She was the Chairman, CEO, and President of the company while on an industrial leave from the University of California, Berkeley. She returned to Berkeley in July 2000, and is currently the Chief Technical Officer of Bandwidth9. Her prior industrial experience includes a five-year tenure at Bellcore from 1987–1992. From 1992–1996, she was at Stanford University, where she was an Associate Professor of electrical engineering. She served as the Program Cochair and the General Cochair of the Conference on Lasers and Electro-Optics (CLEO) in 1997 and 1999, respectively. She served as a LEOS Board of Governor and is a Director-at-Large of the Optical Society of America (OSA). She was a member of the USAF Scientific Advisory Board from 1997–2000. She has coauthored more than 180 papers in technical journals and conferences and has been awarded more than 20 patents. Her research interests include semiconductor optoelectronic devices and materials and their applications.

Dr. Chang-Hasnain is a Fellow of the OSA. She has received numerous awards recognizing her seminal work on VCSEL and diode laser arrays. She was named a Presidential Faculty Fellow by the White House, a National Young Investigator, a Packard Fellow from the David and Lucile Packard Foundation, a Sloan Research Fellow of the Alfred P. Sloan Foundation, and the Outstanding Young Electrical Engineer of the Year by Eta Kappa Nu. She received the 1994 IEEE LEOS Distinguished Lecturer Award. Recently, she was awarded with the 2000Curtis W. McGraw Research Award from the American Society of Engineering Education. She was an Editor of the IEEE CIRCUITS AND DEVICES MAGAZINE and a Guest Editor for the IEEE JOURNAL ON SELECTED TOPICS IN QUANTUM ELECTRONICS special issue on Semiconductor Lasers in 1999.

LaTeX 2_ε